Application of hyperspherical coordinates to two-dimensional charged excitons

2000 J. Phys.: Condens. Matter 12 7905

(http://iopscience.iop.org/0953-8984/12/36/305)

J. Phys.: Condens. Matter **12** (2000) 7905–7914. Printed in the UK PII: S0953-8984(00)15021-0

Application of hyperspherical coordinates to two-dimensional charged excitons

W Y Ruan†, K S Chan‡ and E Y B Pun§

† Department of Applied Physics, South China University of Technology, Guangzhou 510641, People's Republic of China
‡ Department of Physics and Materials Science, City University of Hong Kong, Hong Kong
§ Department of Electronic Engineering, City University of Hong Kong, Hong Kong

E-mail: phwyruan@scut.edu.cn (W Y Ruan)

Received 28 June 2000, in final form 3 July 2000

Abstract. Hyperspherical coordinates are applied to the bound states of two-dimensional charged excitons. The Schrödinger equation is solved by two different methods, i.e., by a direct expansion in hyperspherical harmonics and by separating it into a radial equation and an angular equation on the basis of the adiabatic approximation. Our main findings are: (a) the low-lying eigenenergies scale nearly linearly with the reduced mass of the exciton; (b) the adiabatic approximation produces a ground-state energy of -1.1384 au, which compares well to -1.1164 au, obtained by hyperspherical expansion in the positronium limit.

1. Introduction

Two-dimensional charged excitons in semiconducting quantum wells have been the subject of a great deal of study recently [1–9]. A charged exciton comprises two electrons and one hole (X^-) or two holes and one electron (X^+). Charged excitons are the analogues of positronium ions, known in atomic physics. Already, several variational calculations have been carried out to evaluate the binding energies of charged excitons. Variational calculations can be made accurate by the use of several hundred variational parameters [10]. However, they shed little light on the nature of the wavefunction, and probing the excited states is problematic.

The solution of three-body problems with interactions via the long-range Coulomb force is not an easy task. A comprehensive understanding of the two-electron atomic system was only achieved in recent years [11]. Hyperspherical coordinates provide a suitable framework for understanding the problem. In this paper, we employ this framework to study not only the ground state but also the excited states. Our following discussion is specifically for X^-. Results for X^+ can be obtained by replacing the electrons with holes and the hole with an electron.

2. The Schrödinger equation in hyperspherical coordinates

For one hole and two electrons moving in two space dimensions, the Schrödinger equation is

$$\left[\frac{p_1^2}{2m_e}+\frac{p_2^2}{2m_e}+\frac{p_3^2}{2m_h}+\frac{e^2}{4\pi\epsilon}\left(\frac{1}{|z_{12}|}-\frac{1}{|z_{13}|}-\frac{1}{|z_{23}|}\right)\right]\Psi(z_1,z_2,z_3)=E\Psi(z_1,z_2,z_3) \qquad (1)$$

0953-8984/00/367905+10$30.00

where z_1 and z_2 are respectively the imaginary positions of electrons 1 and 2 in the x–y plane; z_3 is the imaginary position of the hole. When effective atomic units (au) are used, i.e., the unit of energy is $m_e(e^2/4\pi\epsilon\hbar)^2$ and the unit of length is $4\pi\epsilon\hbar^2/(m_e e^2)$, equation (1) can be rewritten more succinctly as

$$\left[-\frac{1}{2}(\nabla_1^2+\nabla_2^2+\sigma\nabla_3^2)+\frac{1}{|z_{12}|}-\frac{1}{|z_{13}|}-\frac{1}{|z_{23}|}\right]\Psi(z_1,z_2,z_3)=E\Psi(z_1,z_2,z_3) \tag{2}$$

where $\sigma = m_e/m_h$.

To separate the trivial centre-of-mass motion from the relative motion, we introduce the centre-of-mass and relative coordinates to describe the system. For a three-body system, there are three different sets of relative coordinates, $\{\eta_1^{(j)}, \eta_2^{(j)}\}$ $(j = a, b, c)$, defined by

$$\begin{aligned}
\eta_1^{(a)} &= \sqrt{\frac{m_1m_2}{m_e(m_1+m_2)}}(z_2-z_1)=\sqrt{\frac{1}{2}}(z_2-z_1)\\
\eta_2^{(a)} &= \sqrt{\frac{(m_1+m_2)m_3}{m_e(m_1+m_2+m_3)}}\left(z_3-\frac{m_1z_1+m_2z_2}{m_1+m_2}\right)=\sqrt{\frac{2}{1+2\sigma}}\left(z_3-\frac{z_1+z_2}{2}\right)\\
\eta_1^{(b)} &= \sqrt{\frac{m_2m_3}{m_e(m_2+m_3)}}(z_3-z_2)=\sqrt{\frac{1}{1+\sigma}}(z_3-z_2)\\
\eta_2^{(b)} &= \sqrt{\frac{(m_2+m_3)m_1}{\mu(m_1+m_2+m_3)}}\left(z_1-\frac{m_2z_2+m_3z_3}{m_2+m_3}\right)=\sqrt{\frac{1+\sigma}{1+2\sigma}}\left(z_1-\frac{\sigma z_2+z_3}{1+\sigma}\right)\\
\eta_1^{(c)} &= \sqrt{\frac{m_3m_1}{m_e(m_3+m_1)}}(z_1-z_3)=\sqrt{\frac{1}{1+\sigma}}(z_1-z_3)\\
\eta_2^{(c)} &= \sqrt{\frac{(m_3+m_1)m_2}{m_e(m_1+m_2+m_3)}}\left(z_2-\frac{m_3z_3+m_1z_1}{m_3+m_1}\right)=\sqrt{\frac{1+\sigma}{1+2\sigma}}\left(z_2-\frac{z_3+\sigma z_1}{1+\sigma}\right)
\end{aligned} \tag{3}$$

where m_1, m_2 and m_3 are masses of particles 1, 2, and 3 respectively. $m_1 = m_2 = m_e$ and $m_3 = m_h$. The corresponding hyperspherical coordinates are defined by

$$\begin{aligned}
&\eta_1^{(j)} = r\cos\phi^{(j)}\exp(\mathrm{i}\varphi_1^{(j)}) \qquad \eta_2^{(j)} = r\sin\phi^{(j)}\exp(\mathrm{i}\varphi_2^{(j)})\\
&(0\leqslant r<\infty;\ 0\leqslant\phi^{(j)}\leqslant\pi/2;\ 0\leqslant\varphi_1^{(j)},\varphi_2^{(j)}\leqslant 2\pi;\ j=a,b,c)
\end{aligned} \tag{4}$$

where $\phi^{(j)}$ is the hyperangle; $\varphi_1^{(j)}$ and $\varphi_2^{(j)}$ are respectively the polar angles of $\eta_1^{(j)}$ and $\eta_2^{(j)}$. The hyperradius r is given by

$$r=\sqrt{|\eta_1^{(a)}|^2+|\eta_2^{(a)}|^2}=\sqrt{|\eta_1^{(b)}|^2+|\eta_2^{(b)}|^2}=\sqrt{|\eta_1^{(c)}|^2+|\eta_2^{(c)}|^2} \tag{5}$$

which measures the size of the system; it is independent of the choice of relative coordinates. Since most of our following discussion holds for any set of coordinates, the superscript (j) of the angular variables $\{\phi^{(j)}, \varphi_1^{(j)}, \varphi_2^{(j)}\}$ will be shown only when necessary.

With an arbitrary set of hyperspherical coordinates $\{r, \phi, \varphi_1, \varphi_2\}$, the Schrödinger equation for the relative motion reads

$$\left[-\frac{1}{2}\left(\frac{\partial^2}{\partial r^2}+\frac{3}{r}\frac{\partial}{\partial r}-\frac{\Lambda^2(\Omega)}{r^2}\right)+\frac{C(\Omega)}{r}\right]\Psi(r,\Omega)=E\Psi(r,\Omega) \tag{6}$$

where

$$\Lambda^2(\Omega)=-\frac{\partial^2}{\partial\phi^2}-\left(\frac{\cos\phi}{\sin\phi}-\frac{\sin\phi}{\cos\phi}\right)\frac{\partial}{\partial\phi}+\frac{\hat{\ell}^2(\varphi_1)}{\cos^2\phi}+\frac{\hat{\ell}^2(\varphi_2)}{\sin^2\phi} \tag{7}$$

is the grand orbital operator, $\hat{\ell}(\varphi_1) = -\mathrm{i}\,\partial/\partial\varphi_1$, etc, and

$$C(\Omega) = \sqrt{\frac{1}{2}}\frac{1}{\cos\phi^{(a)}} - \sqrt{\frac{1}{1+\sigma}}\cos\phi^{(b)} - \sqrt{\frac{1}{1+\sigma}}\cos\phi^{(c)} \tag{8}$$

is the fictitious electric charge. Ω stands for a collective set of the angular variables $\{\phi, \varphi_1, \varphi_2\}$.

The common eigenfunctions of the operators $\{\Lambda^2(\Omega), \hat{\ell}(\varphi_1), \hat{\ell}(\varphi_2)\}$, called the hyperspherical harmonics $Y_{\{\nu l_1 l_2\}}(\Omega)$, are given by

$$Y_{\{\nu l_1 l_2\}}(\Omega) = \Theta_\nu^{l_1 l_2} P_\nu^{l_1 l_2}(\phi)\exp[\mathrm{i}(l_1\varphi_1 + l_2\varphi_2)] \tag{9}$$

where $\Theta_\nu^{l_1 l_2}$ is a normalization constant and $P_\nu^{l_1 l_2}$ is a Jacobi polynomial:

$$\Theta_\nu^{l_1 l_2} = \sqrt{\frac{(2\nu + |l_1| + |l_2| + 1)\nu!(\nu + |l_1| + |l_2|)!}{2\pi^2(\nu + |l_1|)!(\nu + |l_2|)!}} \tag{10}$$

$$P_\nu^{l_1 l_2}(\phi) = \sum_{k=0}^{\nu}(-)^{\nu-k}\binom{\nu + |l_2|}{k}\binom{\nu + |l_1|}{\nu - k}(\cos\phi)^{2k+|l_1|}(\sin\phi)^{2(\nu-k)+|l_2|}. \tag{11}$$

$Y_{\{\nu l_1 l_2\}}(\Omega)$ satisfy the eigenequations

$$\begin{aligned}
&\Lambda^2(\Omega)Y_{\{\nu l_1 l_2\}}(\Omega) = \lambda(\lambda+2)Y_{\{\nu l_1 l_2\}}(\Omega)\\
&\hat{\ell}(\varphi_1)Y_{\{\nu l_1 l_2\}}(\Omega) = l_1 Y_{\{\nu l_1 l_2\}}(\Omega)\\
&\hat{\ell}(\varphi_2)Y_{\{\nu l_1 l_2\}}(\Omega) = l_2 Y_{\{\nu l_1 l_2\}}(\Omega)
\end{aligned} \tag{12}$$

with $\lambda = 2\nu + |l_1| + |l_2|$. For compactness we will use the symbol $[\lambda]$ to denote the full set of quantum numbers $\{\nu, l_1, l_2\}$ in the following. With coordinate set (a), imposing the particle exchange symmetry on $Y_{[\lambda]}(\Omega^{(a)})$ is straightforward, i.e., $l_1 =$ odd for spin-triplet states and $l_1 =$ even for spin-singlet states; with coordinate set (b) and set (c), imposing the exchange symmetry is more complicated [12].

3. A direct diagonalization approach

To obtain the eigenenergies and eigenfunctions from equation (6), we expand the trial wavefunction Ψ in terms of a complete set $\{\Phi_{n,[\lambda]}(r, \Omega)\}$ [13, 14]:

$$\Psi(r, \Omega) = \sum_{n,[\lambda]} C_{n,[\lambda]}\Phi_{n,[\lambda]}(r, \Omega) \tag{13}$$

where

$$\Phi_{n,[\lambda]}(r, \Omega) = \left[\frac{\beta^4 n!}{(n+3)!}\right]^{1/2} L_n^{(3)}(\beta r)\exp(-\beta r/2)Y_{[\lambda]}(\Omega). \tag{14}$$

Here $L_n^{(\gamma)}$ are Laguerre polynomials and β is a variational parameter used to minimize the ground-state energy. $\Phi_{n,[\lambda]}(r, \Omega)$ fulfils the normalization condition

$$\int \left[\Phi_{n,[\lambda]}(r, \Omega)\right]^* \Phi_{n',[\lambda']}(r, \Omega)r^3\,\mathrm{d}r\,\mathrm{d}\Omega = \delta_{n,n'}\delta_{[\lambda],[\lambda']} \tag{15}$$

where $\delta_{[\lambda],[\lambda']} = \delta_{\nu,\nu'}\delta_{l_1,l_1'}\delta_{l_2,l_2'}$, $\mathrm{d}\Omega = \sin\phi\cos\phi\,\mathrm{d}\phi\,\mathrm{d}\varphi_1\,\mathrm{d}\varphi_2$.

Substituting equations (13) into (6), we obtain a matrix eigenequation

$$\underline{\mathbf{H}}\,\underline{C} = E\underline{C} \tag{16}$$

where $\underline{C}$ is a one-column matrix of $C_{n,[\lambda]}$, and $\underline{\mathbf{H}}$ is a square matrix of the Hamiltonian

$$H = -\frac{1}{2}\left(\frac{\partial^2}{\partial r^2} + \frac{3}{r}\frac{\partial}{\partial r} - \frac{\Lambda^2(\Omega)}{r^2}\right) + \frac{C(\Omega)}{r} \tag{17}$$

whose matrix elements can be evaluated analytically by transforming the angular variables of $Y_{[\lambda]}$ from one set into another.

To gain insight into the role played by the variational parameter β, in figure 1 we present the ground-state energies calculated with a number of β-values in the range $1 \leqslant \beta \leqslant 5$; the number of basis elements in the Laguerre polynomials used in the calculations are $N_{LP} = 1, 2, 3, 4, 5,$ and 6, in the positronium limit ($\sigma = 1$). Figure 1 shows the existence of an optimized β-value which minimizes the ground-state energy. The optimized β-value increases slightly as L_{LP} increases. It is clear that when $N_{LP} \geqslant 5$, the calculated ground-state energy converges to a value which is nearly independent of β over a broad range. A more detailed observation reveals that when L_{LP} is sufficiently large, the optimized β-value can be expressed as $2\sqrt{2|E|}$. This coincides with the asymptotic behaviour of the wavefunction Ψ in equation (6), where $\Psi \to \exp[-(2|E|)^{1/2}r]$, as $r \to \infty$.

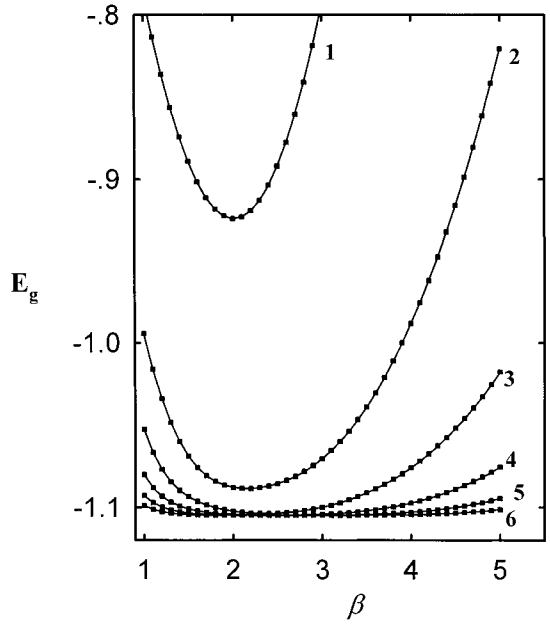

Figure 1. The calculated ground-state energies of a negatively charged exciton as functions of the variational parameter β. The number attached to each curve is the number of Laguerre polynomials used in the calculation. The number of hyperspherical harmonics is fixed at $N_{HH} = 144$.

In table 1, the ground-state energies calculated with different numbers of basis elements are presented to demonstrate the convergence pattern of the expansion in equation (13). When the maximum number of Laguerre polynomials used is $N_{LP} = 8$, the error caused by the truncation in the Laguerre polynomial expansion occurs in the seventh significant number. When the maximum number of hyperspherical harmonics used is $N_{HH} = 256$, the error caused by the truncation of the hyperspherical expansion occurs in the fifth significant figure. Therefore the convergence in the expansion of hyperspherical harmonics is extremely slow compared to that of the radial expansion in Laguerre polynomials.

In figure 2, the four lowest eigenenergies, divided by the absolute ground-state energy of an exciton, are presented as functions of the mass ratio σ. These are the two lowest-energy spin-singlet states with zero angular momentum (denoted by $^1S_1$ and $^1S_2$ respectively), and the two lowest-energy spin-triplet states with zero angular momentum (denoted by $^3S_1$ and $^3S_2$

Table 1. Ground-state ($^1S_1$) energies of X^- in the limit of $\sigma = 1$ obtained by diagonalizing equation (16). N_{LP} is the number of generalized Laguerre polynomials. N_{HH} is the number of hyperspherical harmonics. λ_m is the corresponding maximum λ.

	N_{LP}					
$\lambda_m(N_{HH})$	3	4	5	6	7	8
30(72)	−1.1031896	−1.1046560	−1.1048194	−1.1048297	−1.1048290	−1.1048283
32(81)	−1.1045045	−1.1060808	−1.1062701	−1.1062843	−1.1062839	−1.1062833
34 (90)	−1.1057206	−1.1074068	−1.1076238	−1.1076425	−1.1076427	−1.1076421
36(100)	−1.1070096	−1.1088236	−1.1090748	−1.1090998	−1.1091007	−1.1091002
38(110)	−1.1078493	−1.1097472	−1.1100224	−1.1100520	−1.1100536	−1.1100532
40(121)	−1.1086389	−1.1106203	−1.1109203	−1.1109551	−1.1109574	−1.1109571
42(132)	−1.1094798	−1.1115561	−1.1118857	−1.1119270	−1.1119305	−1.1119302
44(144)	−1.1100476	−1.1121878	−1.1125381	−1.1125842	−1.1125885	−1.1125884
46(156)	−1.1105885	−1.1127921	−1.1131636	−1.1132149	−1.1132201	−1.1132201
48(169)	−1.1111660	−1.1134410	−1.1138370	−1.1138946	−1.1139011	−1.1139012
50(182)	−1.1115676	−1.1138917	−1.1143051	−1.1143673	−1.1143747	−1.1143750
52(196)	−1.1119534	−1.1143263	−1.1147573	−1.1148244	−1.1148328	−1.1148333
54(210)	−1.1123665	−1.1147938	−1.1152449	−1.1153177	−1.1153273	−1.1153281
56(225)	−1.1126607	−1.1151262	−1.1155918	−1.1156688	−1.1156794	−1.1156803
58(240)	−1.1129455	−1.1154490	−1.1159292	−1.1160105	−1.1160221	−1.1160233
60(256)	−1.1132508	−1.1157965	−1.1162931	−1.1163795	−1.1163924	−1.1163937

respectively). It turns out that, to a good approximation, the eigenenergies of these states scale linearly with the ground-state energy of the exciton. To our knowledge, this scaling behaviour was first discovered by Lin [11], for the ground state of 3D Coulombic three-body systems with two identical particles. We confirm here that this is also true for the ground state and the low-lying excited states of 2D systems.

4. The adiabatic approximation

As is shown above, the convergence of the expansion in hyperspherical harmonics is extremely slow. To overcome this difficulty, in this section, we solve the Schrödinger equation (6) by means of a channel expansion [15]:

$$\Psi(r, \Omega) = r^{-3/2} \sum_{\mu} F_\mu(r)\phi_\mu(r, \Omega) \tag{18}$$

where μ is the channel index. The channel wavefunctions $\phi_\mu(r, \Omega)$ are obtained from the eigenvalue problem

$$\hat{U}\phi_\mu(r, \Omega) = U_\mu(r)\phi_\mu(r, \Omega) \tag{19}$$

where

$$\hat{U} = \frac{1}{2}\frac{\Lambda^2 + 3/4}{r^2} + \frac{C(\Omega)}{r}. \tag{20}$$

Equation (19) is equivalent to solving the Schrödinger equation at constant values of r, neglecting the derivatives with respect to r. Therefore, the channel wavefunctions and the channel potential $U_\mu(r)$ depend parametrically on r.

Substituting equation (18) into (6), multiplying equation (6) by $\left[\phi_\mu(r, \Omega)\right]^*$ from the left, integrating over the angular variables, and making use of equation (19), we obtain a set of

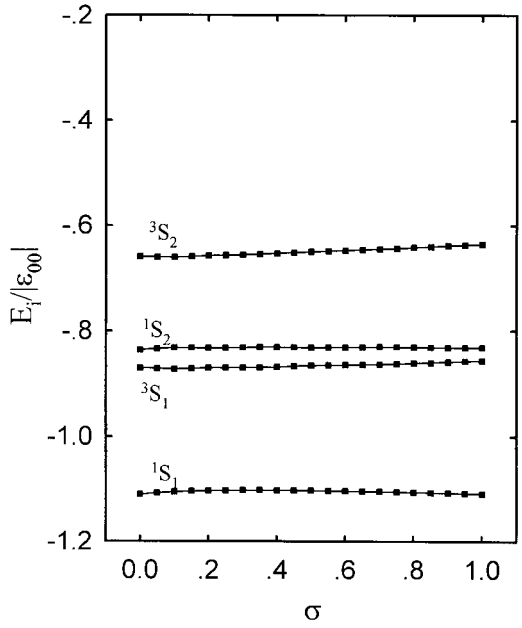

Figure 2. Low-lying eigenenergies of a negatively charged exciton, divided by the absolute ground-state energy of the exciton, $\epsilon_{00} = -2m_1m_3/(m_1 + m_3) = -2/(1 + \sigma)$, are presented as functions of the mass ratio $\sigma = m_e/m_h$. $^1S_1$ and $^1S_2$ ($^3S_1$ and $^3S_2$) denote the two lowest eigenenergy states with $L = 0$ and $S_{\text{spin}} = 0$ ($S_{\text{spin}} = 1$).

coupled equations for determining $\{F_\mu(r)\}$:

$$-\frac{1}{2}\frac{\mathrm{d}^2F_\mu(r)}{\mathrm{d}r^2} + U_\mu(r)F_\mu(r) + \sum_{\mu'} W_{\mu,\mu'}(r)F_{\mu'}(r) = EF_\mu(r) \tag{21}$$

where

$$W_{\mu,\mu'}(r) = -\frac{1}{2}\langle\phi_\mu(r,\Omega)|\partial^2/\partial r^2|\phi_{\mu'}(r,\Omega)\rangle - \langle\phi_\mu(r,\Omega)|\partial/\partial r|\phi_{\mu'}(r,\Omega)\rangle\,\partial/\partial r \tag{22}$$

are the coupling matrix elements.

Since the channel wavefunctions form a complete set, up till now the discussion has been exact. The adiabatic approximation in this context assumes that the channel wavefunctions $\phi_\mu(r,\Omega)$ show only a slow variation with respect to r; that is, to the first order of approximation, we can neglect the channel couplings given by equation (22). In this paper, we confine ourselves to this approximation. The total wavefunction then factorizes according to

$$\Psi_\mu^{ad}(r,\Omega) = F_\mu^{ad}(r)\phi_\mu(r,\Omega). \tag{23}$$

The information regarding the particle correlation is included in the channel functions $\phi_\mu(r,\Omega)$. The radial wavefunctions $F_\mu^{ad}(r)$ and the eigenenergies can be obtained by solving the decoupled equations

$$-\frac{1}{2}\frac{\mathrm{d}^2F_\mu^{ad}(r)}{\mathrm{d}r^2} + U_\mu(r)F_\mu^{ad}(r) = EF_\mu^{ad}(r). \tag{24}$$

The channel potentials $U_\mu(r)$ then have the physical meaning of potentials which control the motion along the coordinate r. In particular, the excited states in a channel represent the excitation of a breathing mode in the system.

As a first step of the approach, we find the channel wavefunctions and channel potentials numerically. In the ranges of small r, $\hat{U}$ is dominated by the term $(\Lambda^2 + 3/4)/r^2$, which describes the centrifugal barrier. The channel wavefunctions are most appropriately expanded in terms of the hyperspherical harmonics:

$$\phi_\mu(r, \Omega) = \sum_{[\lambda]} c^\mu_{[\lambda]}(r) Y_{[\lambda]}(\Omega). \tag{25}$$

In particular, the channel wavefunction $\phi_\mu(r, \Omega)$ converges to a single hyperspherical harmonic $Y_{[\lambda]}(\Omega)$, and the corresponding channel potential $U_\mu(r)$ converges to $[\lambda(\lambda + 2) + 3/4]/r^2$ as $r \to 0$.

In the ranges of large r, the Coulomb term $C(\Omega)/r$ becomes dominant. The channel wavefunctions become localized in the regions where $C(\Omega)$ is minimized (see figure 3). This corresponds to the splittings of the trion into an exciton and a free electron, i.e.,

$$\phi_\mu(r, \Omega) \to \psi_{nl_1l_2}(r, \Omega) = \frac{1}{\sqrt{2}}\left[\phi_{nl_1}(\eta_1^{(b)}) \exp(\mathrm{i}l_2\varphi_2^{(b)}) \pm \phi_{nl_1}(\eta_1^{(c)}) \exp(\mathrm{i}l_2\varphi_2^{(c)})\right] \tag{26}$$

$$U_\mu(r) \to \epsilon_{nl} = -\frac{1}{2(1+\sigma)(n + |l| + 1/2)^2} \tag{27}$$

where ϕ_{nl} is an eigenfunction of an exciton, n is the radial quantum number of a hydrogenic wavefunction, and ϵ_{nl} is the corresponding eigenenergy. '+' is for the spatially symmetric states (spin-singlet states) and '−' is for the spatially antisymmetric states (spin triplet states). The wavefunctions given by equation (26) are difficult to reproduce with a finite set of hyperspherical harmonics. This leads to the slow convergence of the hyperspherical expansion in the above section. It is then most appropriate to expand the channel wavefunctions in terms

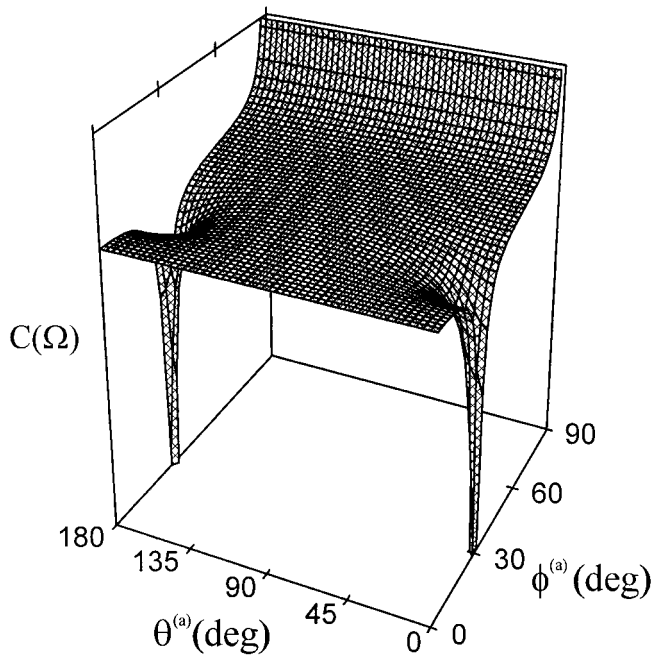

Figure 3. The fictitious electric charge $C(\Omega)$ is presented as a function of $\theta^{(a)}$ and $\phi^{(a)}$.

of $\psi_{nl_1l_2}(r, \Omega)$:

$$\phi_\mu(r, \Omega) = \sum_{nl_1l_2} c^\mu_{nl_1l_2}(r)\psi_{nl_1l_2}(r, \Omega). \tag{28}$$

The channel wavefunctions and channel potentials, calculated with two different basis sets, are matched smoothly at some value of $r_{\mu 0}$.

In figure 4, some low-lying channel potentials are presented for spin-singlet states with zero orbital angular momentum and for systems with $\sigma = 1$. The lowest curve, labelled by $\mu = 0$, is significantly lower than the other curves. It converges to the ground-state energy of an exciton, $\epsilon_{00} = -1$, as $r \to \infty$. In the ranges of small r, it shows a potential well which may support bound states against dissociation.

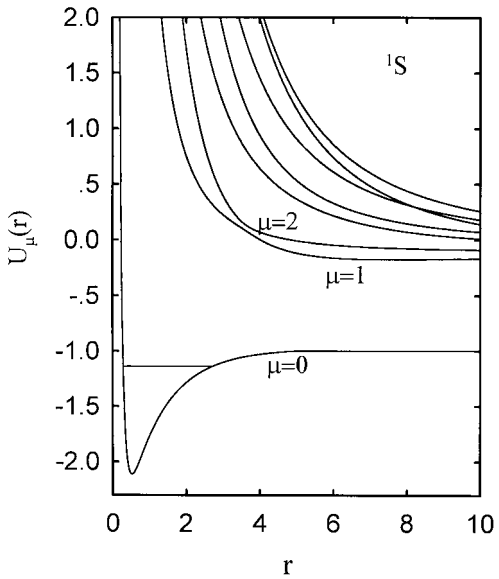

Figure 4. Channel potentials for states ^{1}S of systems with $\sigma = 1$. The lowest curve converges to the ground state of an exciton. Each of the other curves converges to an excited state of an exciton. The horizontal line gives the bound state supported by the lowest curve, which corresponds to the ground state of the system.

With the channel potentials as the input, we solve equation (24) by expanding $F^{ad}_\mu(r)$ in terms of the Laguerre polynomials. With the lowest channel potential we obtain a single bound state with eigenenergy -1.1384, which compares well to -1.1164, the ground-state energy obtained in section 3.

In figure 5, we present the channel potentials for spin-triplet states with zero orbital angular momentum. The lowest curve, which converges to -1, is also significantly lower than the other curves, but the potential well that it shows is too shallow to support any stable bound state against dissociation. In figure 2, all of the spin-triplet states lie beyond the ground state of an exciton in energy. Hence both methods predict no stable bound states with triplet spin.

5. Discussion

In this article, we have used two different methods to evaluate the low-lying quantum spectrum of a 2D Coulombic three-body system. The expansion of the trial wavefunction into a series of

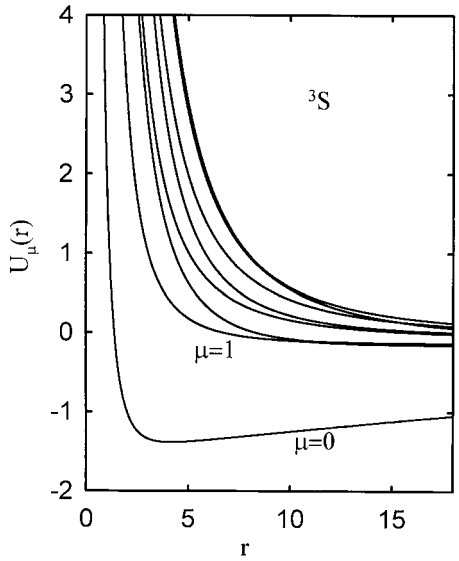

Figure 5. As figure 4, but for ^{3}S states. The lowest curve shows a shallow well insufficient to support a bound state.

products of Laguerre polynomials and hyperspherical harmonics is simple and straightforward for evaluating the eigenfunctions and eigenenergies but suffers from slow convergence in the hyperspherical expansion. The convergence may improve if hydrogenic wavefunctions are included as part of the basis functions. In the adiabatic channel approach, the hyperradius r is treated as a parameter. In the ranges of small r, the wavefunction converges to a hyperspherical harmonic, while in the ranges of large r the wavefunction converges to a hydrogenic wavefunction. Mixings of basis functions occur only in the intermediate region. Hence accurate adiabatic channel potential curves can now be obtained. The adiabatic approach is useful if the mixings of different channels are small. This occurs when a channel potential curve is well separated from the others—such as the lowest curves in figures 4 and 5. In our present system, only the ground state is found to be stable against dissociation. In systems with strong electron–phonon interaction or in a strong magnetic field, more stable bound states can appear. Investigating the high-lying states then becomes practically important.

Acknowledgments

This work was supported by the National Natural Science Foundation, grant No 19875018, People's Republic of China, and also in part by the Guangdong Natural Science Foundation and Guangzhou Natural Science Foundation.

References

[1] Stebe B and Ainane A 1989 *Superlatt. Microstruct.* **5** 545
[2] Kheng, Cox R T, Merle d'Aubigne Y, Bassani F, Saminadayer K and Tatarenko S 1993 *Phys. Rev. Lett.* **71** 1752
[3] Shields A J, Foden C L, Pepper M, Ritchie D A, Grimshaw M P and Jones G A C 1994 *Superlatt. Microstruct.* **15** 355
[4] Finkelstein, Shtrikman H and Bar-Joseph I 1995 *Phys. Rev. Lett.* **74** 976
[5] Shields A J, Osborne J L, Simmons M Y, Pepper M and Ritchie D A 1996 *Phys. Rev.* B **53** 13 002

[6] Thilagam A 1997 *Phys. Rev.* B **55** 7804
[7] Ruan W Y, Chan K S, Ho H P, Zhang R Q and Pun E Y B 1999 *Phys. Rev.* B **60** 5714
[8] Xie W F and Chen C Y 1998 *Solid State Commun.* **107** 439
[9] Riva C, Peeters F M and Varga K 2000 *Phys. Rev.* B **61** 13 873
[10] Varga K 1998 *Phys. Rev.* B **57** 1330
[11] Lin C D 1995 *Phys. Rep.* **257** 2
[12] Ruan W Y and Bao C G 1997 *J. Math. Phys.* **38** 5634
[13] Zhang R Q 1996 *Int. J. Quantum Chem.* **59** 203
[14] Zhang R Q and Deng C H 1993 *Phys. Rev.* A **47** 71
[15] Macek J H 1968 *J. Phys. B: At. Mol. Phys.* **1** 831